Int. J. Electrochem. Sci., 15 **(2020)** 11416 – 11426, doi: 10.20964/2020.11.15

International Journal of
ELECTROCHEMICAL
SCIENCE
www.electrochemsci.org

Application of Gold Nanoparticles and Nano-Diamond Modified Electrode for Hemoglobin Electrochemistry

Hui Cheng[1,2], *Yunxiu Sun*[1], *Bo Shao*[2], *Ying Deng*[2], *Xiaoping Zhang*[2,*], *Guangjiu Li*[1*], *Wei Sun*[2]

[1] Key Laboratory of Optic-electric Sensing and Analytical Chemistry for Life Science of Ministry of Education, Shandong Key Laboratory of Biochemical Analysis, College of Chemistry and Molecular Engineering, Qingdao University of Science and Technology, Qingdao 266042, P R China
[2] Key Laboratory of Laser Technology and Optoelectronic Functional Materials of Hainan Province, College of Chemistry and Chemical Engineering, Hainan Normal University, Haikou 571158, P R China
[*]E-mail: 254787885@qq.com and lgjqust@126.com

Received: 25 June 2020 / *Accepted:* 13 August 2020 / *Published:* 30 September 2020

In this paper nano-diamond (ND) decorated carbon ionic liquid electrode (CILE) was constructed by drop-casting, which was further modified by electrodeposited gold nanoparticles (AuNPs), hemoglobin (Hb) and Nafion orderly to obtain an electrochemical biosensor (Nafion/Hb/AuNPs/ND/CILE). The morphology of AuNPs/ND composite was checked by scanning electron microscopy. A pair of redox peaks of Hb on the modified electrode with good reversibility and symmetry appeared in cyclic voltammograms . The effects of pH and scan rate on Hb electrochemistry were further investigated to calculate the electrochemical parameters. The Hb based biosensor showed excellent electrocatalytic ability to the reduction of various substrates such as sodium nitrite, trichloroacetic acid and potassium bromate with the detection range from 0.07 to 2.60 mmol L^{-1}, 1.00 to 500.00 mmol L^{-1} and 0.35 to 12.00 mmol L^{-1}, respectively. Nafion/Hb/AuNPs/ND/CILE showed good reproducibility and stability, which was applied to the analysis $KBrO_3$ content in real sea water samples.

Keywords: Gold nanoparticle; Nano-diamond; Electrochemistry; Carbon ionic liquid electrode; Hemoglobin.

1. INTRODUCTION

Electrochemical enzyme biosensors are powerful analytical tools with the advantages including portability, self-contained and low-cost, which are now widely used in the detection of various analytes [1, 2]. However, the deeply present of redox-active center of protein is not favorable to the transfer of electrons between bare electrodes[3]. Therefore, the electron transfer of redox proteins was realized by modifying the electrodes with different materials [4-8].

Electrochemical analysis based on advanced nanomaterials exhibits excellent sensitivity, selectivity and fast response, which is vital in the fields of biomedical and analytical science [9]. Among the various nano-allotropes of the carbon family, nano-diamond (ND) has attracted many attentions during the past decade due to the specific properties, including excellent optical properties, high electrochemical potential energy, good biocompatibility and chemical stability. Because of these novel properties, various sensor platforms have been built with ND. For example, Shahrokhian et al. investigated ND-graphite/CTS modified electrode to sensitive detect azathioprine [10]. Babadi et al. prepared ND, carbon nanotube and copper modified electrode to catalyze the amino acids detection [11]. Functionalized ND membrane was utilized for modified electrode by Villalba et al. to detect glucose [12]. Yu et al. fabricated the graphene oxide/ND modified Au electrode as an humidity sensor with ultrahigh performance [13]. Xie et al. fabricated an ND modified enzyme sensor for sensitive determination of trichloroacetic acid (TCA) [14].

Gold nanoparticles (AuNPs) have been extensively used in analytical chemistry due to the unique physical and chemical properties with excellent biocompatibility. AuNPs can be selectively combined with a variety of organic or biological ligands to detect small molecules and biological targets. In the past researches, the emergence of AuNPs as a sensing element has been established a wide range of innovative methods for rapid and effective detection. Zeng et al. sorted out the applications of AuNPs in biosensors[15]. Rasheed et al. discussed the use of AuNPs as labels and substrate materials in various electrochemical DNA sensors [16]. Liu et al. constructed the Au nanocages modified electrode to detect rutin [17].

In this work, a carbon ionic liquid electrode (CILE) was constructed with N-hexylpyridinium hexafluorophosphate ($HPPF_6$) as the modifier [18], which was further modified by ND, AuNPs, hemoglobin and Nafion successively to get the modified electrode (Nafion/Hb/AuNPs/ND/CILE). The excellent electrochemical behaviors of Hb on the modified electrode were obtained, which indicated that a direct and accelerated electron transfer of Hb was realized. The modified electrode was further investigated to detect sodium nitrite ($NaNO_2$), TCA and potassium bromate ($KBrO_3$) sensitively.

2. EXPERIMENTAL

2.1 Chemicals

A CHI 660D electrochemical analyzer (Shanghai CH Instrument, China) was used for electrochemical investigation. A conventional three-electrode system was used with an Hb modified electrode as the working electrode, a platinum wire as the auxiliary electrode and a saturated calomel electrode (SCE) as the reference electrode. Scanning electron microscopic (SEM) images were obtained on JSM-7600F instrument (JEOL, Japan). UV-5 ultraviolet-visible (UV-vis) spectrophotometer (Mettler Toledo, USA) and Nicolet 6700 FT-IR spectrophotometer (Thermo Fisher Scientific Inc., USA) were used for spectroscopic investigations.

2.2 Apparats

ND powder (Nanjing XFNANO Materials Tech. Ltd. Co., China), $HAuCl_4$ (Tianjin Kaima Biochem. Ltd. Co., China), Nafion (5.0–5.4 wt%, Dupont, USA), Hb (Sigma-Aldrich Co., USA), $HPPF_6$ (Lanzhou Yulu Fine Chem. Ltd. Co., China), TCA (Tianjin Kemiou Chemical Ltd. Co., China), $NaNO_2$ (Yantai Sanhe Chem. Ltd. Co., China) and $KBrO_3$ (Shanghai Aladdin Reagent Ltd. Co., China) were used as received. The supporting electrolyte was 0.1 mol L^{-1} phosphate buffer solution (PBS), which was deoxygenized by N_2 before experiment. All reagents were of analytical grade.

2.3 Preparation of modified electrode

CILE was fabricated based on the reference [19]. Then 8.0 μL of 0.5 mg mL^{-1} ND dispersion was spread on the surface of CILE. After natural drying, AuNPs was loaded on the ND modified electrode surface with electrodeposition method in 1.0 mmol L^{-1} $HAuCl_4$ solution (deposition potential of -0.3 V and deposition time of 150 s). Finally, the modified electrode (Nafion/Hb/AuNPs/ND/CILE) was prepared by applying 8.0 μL of 15 mg mL^{-1} Hb and 6.0 μL of 0.5% Nafion solution on the electrode surface step-by-step, which was stored in 4° C before used.

3. RESULTS AND DISCUSSION

3.1. SEM images

The morphologies of materials on the electrode are shown in Fig. 1. ND exhibited as sphere at the average diameter of 60 nm with some accumulation (Fig. 1A). Fig. 1B shows that AuNPs had good dispersion and uniform sphere with the average diameter as 80 nm. In Fig. 1C, AuNPs were loaded on the ND surface after electrodeposition with the thick film present. Electrodeposition is a commonly used procedure for the directly formation of AuNPs on the electrode surface, which has been used for the electrode modification and electrochemical applications [20,21].

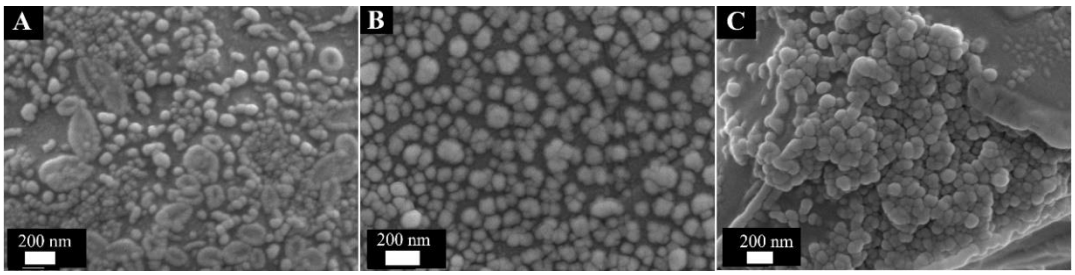

Figure 1. SEM images of (A) ND/CILE; (B) AuNPs/CILE; (C) AuNPs/ND/CILE.

3.2 Spectroscopic results

UV-Vis absorption spectroscopy is often employed to investigate secondary biostructure of the proteins. The position of the protein absorption Soret band can be used to judge whether the structure of Hb is changed [22]. Fig. 2A shows the UV-Vis absorption spectra of Hb in water (curve a) and Hb-ND mixture solution (curve b), which gave the same typical Soret band of heme protein at 405 nm. Therefore Hb had not been denatured in the ND dispersion solution, maintaining the original structure and biological activity. The completeness of the secondary structure of the proteins is also checked by FI-IR spectroscopy, which can offer the spectroscopic date of protein. As shown in Fig. 2B, the characteristic peaks of Hb (b) were located at 1654 cm^{-1} and 1537 cm^{-1}, which were in consistent with the characteristic peaks of Hb-ND mixture (a) at 1652 cm^{-1} and 1539 cm^{-1}, indicating Hb remained biostructure within the mixture.

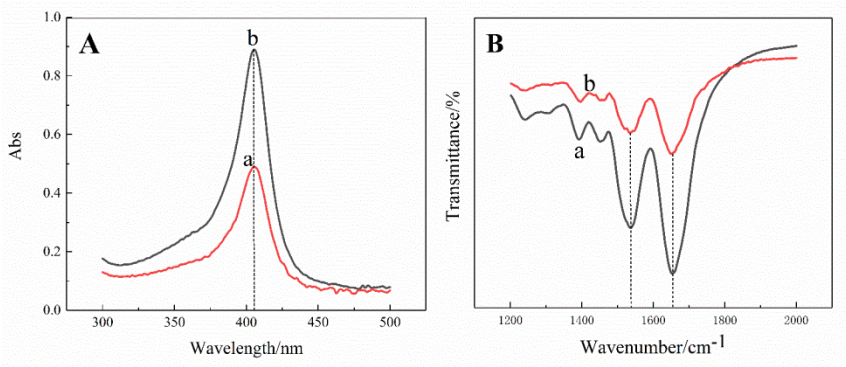

Figure 2. (A) UV-Vis absorption spectra of Hb (a) and Hb-ND mixture (b); (B) FT-IR spectra of Hb-ND mixture (a) and Hb (b).

3.3 Electrochemical characterization

Electrochemical response of AuNPs/ND/CILE in potassium ferricyanide solution was investigated by cyclic voltammetry with results in Fig. 3A, which showed an enhanced current response compared with those of ND/CILE and CILE. Detailed electrochemical parameters of three electrodes were summarized in table 1. Owing to excellent electrochemical property of ND and AuNPs, the presence of ND and AuNPs gave positive effects to the electron transfer with the increase of the peak currents and the decrease of the peak-to-peak potential. Then the effective surface area of AuNPs/ND/CILE was further investigated by cyclic voltammetry at different scan rates from 0.01 V s^{-1} to 1.00 V s^{-1}. As can be seen in Fig. 3B, the redox peak current and potential both changed with the increase of scan rate. The linear relationships between Ip and the square-root of scan rate ($\upsilon^{1/2}$) was got with the equations as Ipc(μA)= 172.96 $\upsilon^{1/2}$ + 160.01 (n=21, γ=0.998) and Ipa (μA)= -149.82 $\upsilon^{1/2}$ + 263.38 (n=21, γ=0.993), which indicated the redox reaction was a diffusion-controlled process. Based on the Randles-Servick equation [23], the effective surface area of AuNPs/ND/CILE was calculated as 0.252 cm^2, which was larger than that of CILE (0.144 cm^2) [24], indicating that the existence of spherical AuNPs and ND could greatly improve the effective surface area of the modified electrode.

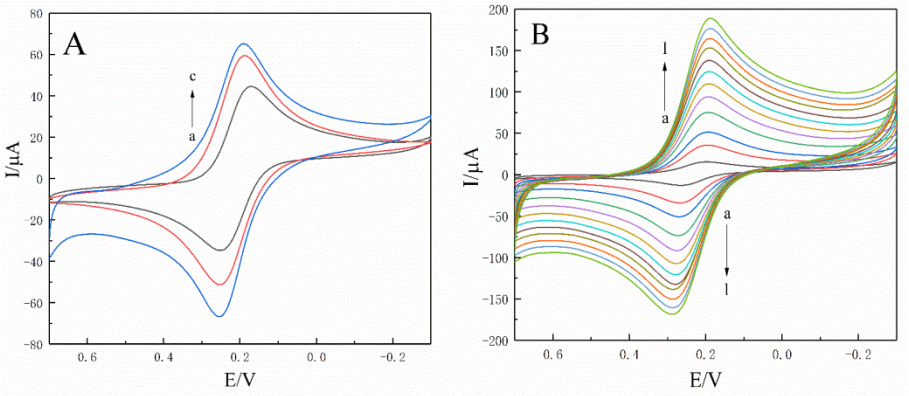

Figure 3. Cyclic voltammograms in 1.0 mmol L^{-1} $K_3[Fe(CN)_6]$ and 0.50 mol L^{-1} KCl solution of (a) CILE, (b) ND/CILE and (c) AuNPs/ND/CILE; (B) cyclic voltammograms of AuNPs/ND/CILE at different scan rates (a to l as 0.01, 0.05, 0.10, 0.20, 0.30, 0.40, 0.50, 0.60, 0.70, 0.80, 0.90, 1.00 V s^{-1}).

Table 1. Electrochemical parameters of different electrodes.

Electrode	Epa (V)	Epc (V)	Ipa (μA)	Ipc (μA)	ΔEp (mV)	Ipa/Ipc
CILE	0.252	0.172	41.04	44.90	80	0.914
ND/CILE	0.254	0.187	55.36	58.19	67	0.951
AuNPs/ND/CILE	0.254	0.192	64.18	66.53	62	0.964

3.4 Direct electrochemistry of Hb

As described in Fig. 4, electrochemical behaviors of various modified electrodes were investigated. No electrochemical responses could be observed on Nafion/CILE (curve a) and Nafion/AuNPs/ND/CILE (curve b), showing no electrochemical reaction occurred on the electrode surface. However, the existence of AuNPs and ND increased the effective surface area and the corresponding background current with the increase of interfacial electric double layer. It is seen that a pair of redox peaks appeared on Nafion/Hb/CILE (curve c), indicating that electron transfer happened between Hb and CILE. That is, Hb can undergo the electron transfer between the heme active center and the electrode. Excellent chemical stability, rapid ionic conductivity and stable electrochemical windows of CILE can promote the appearance of redox peaks [25]. On Nafion/Hb/AuNPs/ND/CILE (curve d), the redox peak currents enhanced with the peak shape more symmetry, which proved the existence of AuNPs and ND offered an efficient electron transfer route for Hb with the electron transfer rate accelerated. The value of Epc and Epa were got as at -0.206 V and -0.128 V, respectively, with the peak-to-peak separation (ΔEp) as 78 mV and the formal potential ($E^{0'}$) as -0.167 V (vs. SCE). Also the peak currents Ipc and Ipa were got as 49.81 μA and 44.23 μA, respectively, with Ipc/Ipa as 1.13. All the date proved that the characteristic electrochemical behavior of Hb heme Fe(III)/Fe(II) was realized with an approximately reversible process.

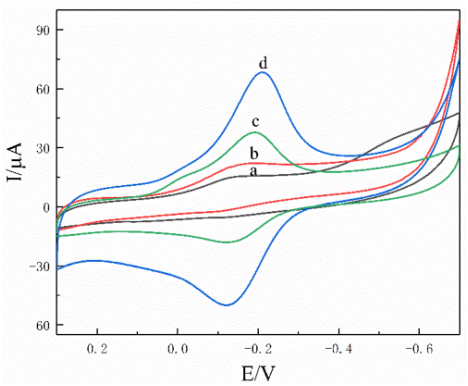

Figure 4. Cyclic voltammograms of (a) Nafion/CILE, (b) Nafion/AuNPs/ND/CILE, (c) Nafion/Hb/CILE, (d) Nafion/Hb/AuNPs/ND/CILE in pH 2.0 PBS with scan rate as 0.10 mV s^{-1}.

3.5 Effect of scan rate and pH

As shown in Fig. 5A, electrochemical responses of Nafion/Hb/AuNPs/ND/CILE were studied in the scan rate range of 0.05 V s^{-1} to 1.00 V s^{-1}. A pair of the symmetric redox peaks appeared and the redox peak currents increased gradually with the increase of scan rate. Two linear regression equations were established as Ipa (μA)= -177.61 υ (V s^{-1})–28.73 (n=16,γ=0.992) and Ipc (μA)= 192.10 υ (V s^{-1}) + 4.35 (n=16, γ=0.992), respectively. The results indicated the electrochemical behavior of Hb was a typical interface-dominated process. ΔEp was also increased with two straight lines got as Epc (V)= -0.054 lnυ (V s^{-1}) - 0.27 (n=11, γ=0.996) and Epa (V)= 0.047 lnυ (V s^{-1}) - 0.077 (n=11, γ=0.984), respectively. Electrochemical parameters such as electron transfer number (n), the electron transfer coefficient (α) and heterogeneous electron transfer rate constant (k_s) was computed as 1.030, 0.464 and 2.533 s^{-1}, respectively, based on the Laviron's equation [26]. Compared with the value of k_s with other literatures such as Nafion/GR-MWCNTs/CILE (0.97 s^{-1}) [4], CTS/Fe_3O_4/CILE (0.478 s^{-1}) [27], and GO-Pt/CILE (0.584 s^{-1}) [28], the results proved AuNPs/ND composite had an excellent electron transfer rate. Therefore the high electrical conductivity and biocompatibility of AuNPs, wide electrochemical window and excellent chemical stability of ND provided interface for Hb immobilization, which caused the fast electron transfer on AuNPs/ND composite modified electrode.

To further investigate the influence of solution pH on the direct electrochemistry of Hb, cyclic voltammograms of Hb were obtained in the range of pH 2.0 to 8.0. As can be seen in Fig. 5B, the redox peak potential moved towards the negative direction with the increase of pH, indicating that protons involved in the electrochemical process. Meanwhile the formal peak potential ($E^{0'}$) had a linear relationship with the buffer pH and the equation was $E^{0'}$ (V)= -0.044 pH - 0.056 (n=7, γ=0.992). The slope of -44.4 mV/pH was smaller than the theoretical value of -59.0 mV/pH for a one-electron one-proton reaction [29]. Also it was observed that a largest reduction peak current was got in pH 2.0, which was selected as the electrolyte for further electrocatalytic experiments.

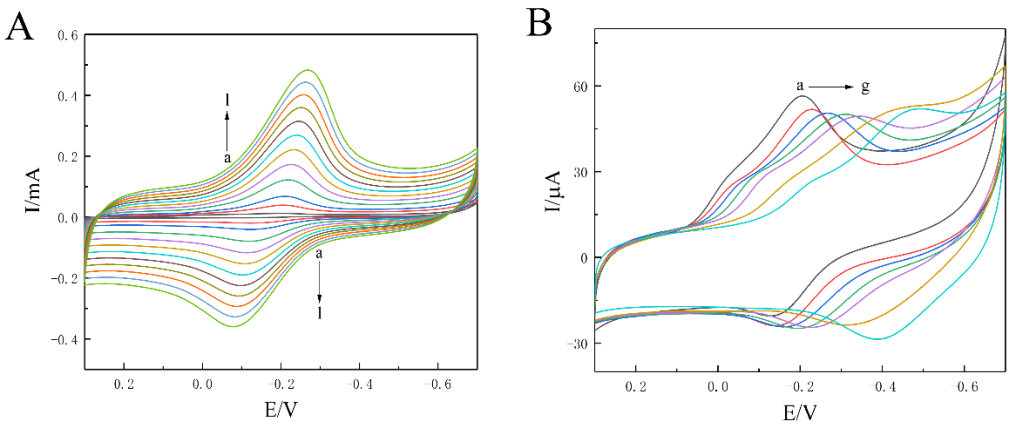

Figure 5. Cyclic voltammograms of Nafion/Hb/AuNPs/ND/CILE in (A) pH 2.0 PBS with the scan rates (from a to l as 0.01, 0.05, 0.10, 0.20, 0.30, 0.40, 0.50, 0.60, 0.70, 0.80, 0.90, 1.00 V s^{-1}); (B) different pH (from a to g as 2.0, 3.0, 4.0, 5.0, 6.0, 7.0, 8.0) with the scan rates of 100 mV s^{-1}.

3.6 Electrocatalytic behaviors

Hb possesses a redox center similar as that of peroxidase, which can catalyze reduction on substrates, such as TCA, $NaNO_2$ and $KBrO_3$, to evaluate the performance of the Hb modified electrode.

TCA is often acted as an herbicide in agriculture and horticulture, and as a preservative in daily drinking water, which can cause environmental pollution. Therefore, the sensitive detection of TCA is of great significance [30]. Thus, the electrocatalytic reduction of TCA in pH 2.0 PBS was studied. As can be seen in Fig. 6A, the reduction peak current increased and the corresponding oxidation peak gradually decreased until to disappear with the increase of TCA concentration. The electrocatalytic reactions involve the reduction of Hb Fe(III) to Hb Fe(II), the reduction of TCA with Hb Fe(II) on the electrode, the reduction of di- chloroacetic and mono-chloroacetic acid with Hb Fe(II) and the reoxidation of Hb Fe(I). Subsequently, the regression equation was got as Ipc (μA) = 1.431 C (mmol L^{-1}) + 79.125 (n=31, γ=0.993) between the reduction peak current and TCA concentration in the range of 1.00 to 100.0 mmol L^{-1}. The detection limit was got as 0.33 mmol L^{-1} (3σ) and the Michaelis-Menten constant (K_M^{app}) was calculated 90.52 mmol L^{-1} based on the Lineweaver-Burk equation [31, 32].

$NaNO_2$ can produce carcinogens when it enters the human body, which is harmful to health. According to the standard of GB 2760, the residual amount of NO_2^- in meat cannot exceed 0.03 g Kg^{-1}. Therefore, a fast, sensitive and efficient method for $NaNO_2$ detection is essential to establish. As described in Fig. 6B, a new catalytic reduction peak at -0.564 V (vs. SCE) appeared at cyclic voltammogram, which indicated the electrocatalytic reaction took place. The catalytic reduction peak value was correspondingly improved with the increase of $NaNO_2$ concentration in the range of 0.07 to 0.30 mmol·L^{-1} and 0.35 to 2.60 mmol·L^{-1}. Two linear regression equations were calculated as Ipc (μA)= 231.570 C (mmol L^{-1}) + 9.610 (n=14, γ=0.994) and Ipc (μA)= 81.130 C (mmol L^{-1}) + 68.150 (n=13, γ=0.994), respectively, with the detection limit as 0.027 mmol·L^{-1} (3σ). The K_M^{app} value was

calculated as 12.06 mmol·L^{-1}. Meanwhile the comparisons of analytical parameters for $NaNO_2$ with different modified electrodes were listed in table 2, which showed that this electrode had high sensitivity for the detection of $NaNO_2$.

Table 2. Comparison of different modified electrodes for $NaNO_2$ detection

Electrodes	Linear range (mmol L^{-1})	LOD (mmol L^{-1})	References
Nafion/HRP/WS_2/CILE	1.50~4.00	0.20	[33]
CNF/Hemin/GCE	5.00~250	0.32	[34]
Nafion/HRP/Co_3O_4NP/CILE	0.10~1.10	0.20	[35]
RGO/GCE	8.90~167	1.00	[36]
Nafion/Hb-Pd-GR/CILE	0.6~61.0	0.35	[37]
CTS/Mb/SWCNHs/CILE	0.04~0.74	0.13	[38]
CTS/ELDH-GR-Hb/CILE	5.0-360	1.51	[39]
Nafion/Mb-HAp@CNF/CILE	0.30~10.00	0.23	[40]
Nafion/Hb/AuNPs/ND/CILE	0.07~2.60	0.027	This work

Notes: GR: graphene; RGO: reduced graphene oxide, GCE: glassy carbon electrode, Hap: hydroxyapatite, CNF: carbon nanofiber, WS_2: tungsten disulfide, Mb: myoglobin, HRP: horseradish peroxidase; SWCNHs: single-walled carbon nanohorn; ELDH: exfoliated Co_2Al layered double hydroxide; CTS: chitosan.

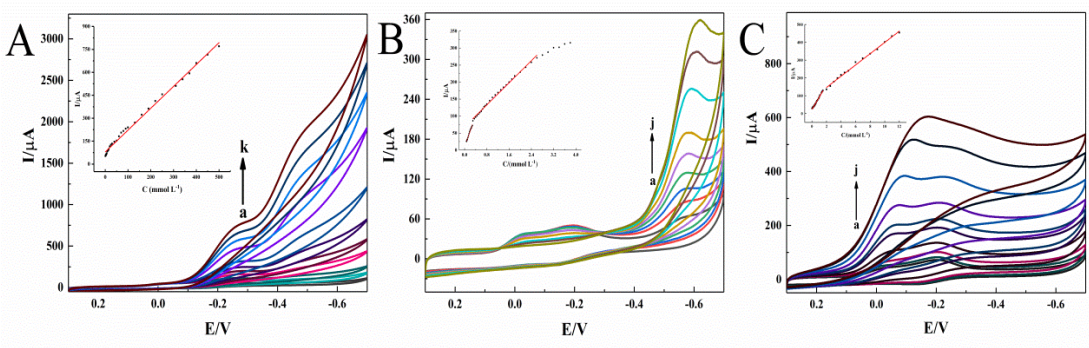

Figure 6. CVs of Nafion/Hb/AuNPs/ND/CILE with different concentrations of (A) TCA (from a to k as: 1.00, 5.00, 11.0, 30.0, 50.0, 80.0, 130, 220, 280, 340, 400 mmol L^{-1}); inset is the linear relationship of cathodic current versus TCA concentration; (B) $NaNO_2$ (from a to j as: 0.07, 0.16, 0.24, 0.35, 0.55, 0.80, 1.40, 2.00, 2.60 mmol·L^{-1}); inset is the linear relationship of cathodic current versus $NaNO_2$ concentration; (C) $KBrO_3$ (from a to j as: 0.01, 0.10, 0.35, 0.70, 1.50, 2.0, 3.50, 6.00, 9.00, 12.00 mmol·L^{-1}); inset is the linear relationship of cathodic current versus $KBrO_3$ concentration.

$KBrO_3$ is mainly used as analytical reagent, oxidant and food additive. Drinking water containing $KBrO_3$ for a long time will cause the animal's kidney and thyroid to become cancerous. Also the World Health Organization restricts the $KBrO_3$ content in water to 0.01 mg L^{-1} in 2004 [41]. Therefore, the detection of $KBrO_3$ in water is also more important. Electrocatalytic reduction of $KBrO_3$ is further checked and shown in Fig. 6C. Two linear relationships between the reduction peak current

and $KBrO_3$ concentration were got in the range of 0.01 to 0.30 mmol·L^{-1} and 0.35 to 12.00 mmol L^{-1} with the regression equation as Ipc (μA)= 0.068 C (mmol L^{-1}) + 0.024 (n=9, γ=0.995) and Ipc (μA)= 0.032 C (mmol L^{-1}) + 0.083 (n=14, γ=0.995), respectively. The detection limit was got as 0.0033 mmol L^{-1} (3σ) with K_M^{app} as 27.32 mmol L^{-1}.

3.7 Sample detection

Seawater sample was collected from Guilinyang Beach of Haikou city, which was filtered and used in the test. Then the different standard $KBrO_3$ solutions were added into the sample solutions and the results were calculated by the calibration curve with the recovery by the standard addition method. As can be seen in table 3, the determination results were desirable with the recoveries in the range of 91.00% to 101.00%, which proved the practical application in water sample detection.

Table 3. Analytical results of $KBrO_3$ concentrations in seawater samples (n=3)

Sample	Detected (mmol L^{-1})	Added (mmol L^{-1})	Total (mmol L^{-1})	Recovery (%)
Seawater	0	1.00	0.91	91.00
		2.00	1.98	99.00
		3.00	3.03	101.00

3.8 Reproducibility and stability of the modified electrode

The reproducibility of Nafion/Hb/Au/ND/CILE for the determination of 1.00 mmol L^{-1} $NaNO_2$ was studied by making 10 modified electrodes independently, which showed a relative standard deviation (RSD) of 4.8%. The stability of the modified electrode was investigated by cyclic voltammetry in pH 2.0 PBS. After 40 circles, the redox peak currents were decreased approximately 4.26% and 80 circles with the decrease of 8.72%. And after two weeks stored at 4 ℃, the peak current maintained 90.0% of the initial value. These results indicated the modified electrode had good biocompatibility and stability.

4. CONCLUSION

In this study AuNPs and ND were used as modifiers to fabricate a sensing platform, which was studied for the electrochemical behavior of Hb. The existence of AuNPs and ND increased the effective surface area and the electron transfer rate on the modified electrode, which provided a guarantee for excellent electrocatalytic performance. Then, the electrocatalysis to $NaNO_2$, TCA and $KBrO_3$ was studied, which showed excellent stability, wider linear range and lower detection limit. According to the above results, AuNPs and ND were benefit for electrode modification and signal amplification, and the modified electrode had potential prospects in electrochemical sensing.

ACKNOWLEDGMENTS
This project was supported by the Hainan Provincial Natural Science Foundation of China (2018CXTD336), the National Natural Science Foundation of China (61864002), Open Project of Chemistry Department of Qingdao University of Science and Technology (QUSTHX201935), and Postgraduate Innovative Research Project of Hainan Normal University (Hsyx2018-9).

References

1. G. Maduraiveeran, M. Sasidharan, V. Ganesan, *Biosens. Bioelectron*., 103 (2018) 113.
2. H. Xie, J. Liu, Z. Wen, G. Luo, Y. Niu, X. Li, G. Li, W. Sun, *Int. J. Electrochem. Sci.*, 14 (2019) 7663.
3. Y. Niu, J. Liu, W. Chen, C. Yin, W. Weng, X. Li, X. Wang, G. Li, W. Sun, *Anal. Methods*, 10 (2018) 5297.
4. W. Sun, L. Cao, Y. Deng, S. Gong, F. Shi, G. Li, Z. Sun, *Anal. Chim. Acta*, 781 (2013) 41.
5. X. Li, X. Niu, W. Zhao, W. Chen, C. Yin, Y. Men, G. Li, W. Sun, *Electrochem. Commun*., 86 (2018) 68.
6. F. Shi, W. Zheng, W. Wang, F. Hou, B. Lei, Z. Sun, W. Sun, *Biosens. Bioelectron*., 64 (2015) 131.
7. W. Sun, Y. Guo, X. Ju, Y. Zhang, X. Wang, Z. Sun, *Biosens. Bioelectron*., 42 (2013) 207.
8. S. Wei, H. Fei, S. Gong, H. Lin, W. Wang, S. Fan, J. Xi, X. Wang, G. Li, *Sens. Actuators* B, 219 (2015) 331.
9. X. Chen, G. Wu, Y. Jiang, Y. Wang, X. Chen, *Analyst*, 136 (2011) 4631.
10. S. Shahrokhian, M. Ghalkhani, *Electrochim. Acta*, 55 (2010) 3621.
11. F. E. Babadi, S. Hosseini, A. Shavandi, H. Moghaddas, A. Shotipruk, S. Kheawhom, *J. Environ. Chem. Eng.*, 7 (2019) 102979.
12. P. Villalba, M. K. Ram, H. Gomez, A. Kumar, V. Bhethanabotla, A. Kumar, *Mater. Sci. Eng*. C, 31 (2011) 1115.
13. X. Yu, X. Chen, X. Ding, X. Chen, X. Yu, X. Zhao, *Sens. Actuators* B, 283 (2019) 761.
14. H. Xie, X. Li, G. Luo, Y. Niu, R. Zou, C. Yin, S. Huang, W. Sun, G. Li, *Diamond Relat. Mater*., 97 (2019) 107453.
15. S. Zeng, K. T. Yong, I. Roy, X. Q. Dinh, X. Yu, F. Luan, *Plasmonics*, 6 (2011) 491.
16. P. A. Rasheed, N. Sandhyarani, *Microchim. Acta*, 184 (2017) 981.
17. J. Liu, W. Weng, C. Yin, X. Li, Y. Niu, G. Li, W. Sun, *J. Chin. Chem. Soc*., 66 (2019) 1336.
18. W. Wang, Y. Cheng, L. Yan, H. Zhu, G. Li, J. Li, W. Sun, *Anal. Methods*., 7 (2015) 1878.
19. W. Chen, W. Weng, X. Niu, X. Li, Y. Men, W. Sun, G. Li, L. Dong, *J. Electroanal. Chem*., 823 (2018) 137.
20. X. Niu, Z. Wen, X. Li, W. Zhao, X. Li, Y. Huang, Q. Li, G. Li, W. Sun, *Sens. Actuators* B, 255 (2018) 471.
21. F. Shi, J. Xi, F. Hou, L. Han, G. Li, S. Gong, C. Chen, W. Sun, *Mater. Sci. Eng*, C, 58 (2016) 450.
22. K. Rosenheck, P. Doty, *P. Natl. A. Sci*., 47 (1961) 1775.
23. A. J. Bard, L. R. Faulkner, *Angew. Chem. Int. Ed*., 41 (2002) 655.
24. W. Sun, P. Qin, H. Gao, G. Li, K. Jiao, *Biosens. Bioelectron*., 25 (2010) 1264.
25. X. Niu, W. Chen, X. Wang, Y. Men, Q. Wang, W. Sun, G. Li, *Mikrochim. Acta*, 185 (2018) 167.
26. E. Laviron, *J. Electroanal. Chem*., 101 (1979) 19.
27. W. Sun, Z. Sun, L. Zhang, X. Qi, G. Li, J. Wu, M. Wang, *Colloids. Surf. B*, 101 (2013) 177.
28. W. Sun, L. Li, B. Lei, T. Li, X. Ju, X. Wang, G. Li, Z. Sun, *Mater. Sci. Eng*, C, 33 (2013) 1907.
29. H. Liu, K. Guo, J. Lv, Y. Gao, C. Duan, L. Deng, Z. Zhu, *Sens. Actuators B*, 238 (2017) 249.
30. H. K. Bhat, M. F. Kanz, G. A. Campbell, G. a. S. Ansari, *Fundam. Appl. Toxicol*., 17 (1991) 240.
31. H. Lineweaver, D. Burk, *J. Am. Chem. Soc*., 56 (1934) 658.
32. K. A. Johnson, R. S. Goody, *Biochemistry,* 50 (2011) 8264.

33. Y. Niu, R. Zou, H. A. Yones, X. Li, X. Li, X. Niu, Y. Chen, P. Li, W. Sun, *J. Chin. Chem. Soc*., 65 (2018) 1127.
34. F. Valentini, L. Cristofanelli, M. Carbone, G. Palleschi, *Electrochim. Acta*, 63 (2012) 37.
35. W. Chen, W. Weng, C. Yin, X. Niu, G. Li, H. Xie, J. Liu, W. Sun, *Int. J. Electrochem. Sci*., 13 (2018) 4741.
36. V. Mani, A. P. Periasamy, S. M. Chen, *Electrochem. Commun*., 17 (2012) 75.
37. W. Chen, X. Niu, X. Li, X. Li, G. Li, B. He, Q. Li, W. Sun, *Mater. Sci. Eng*. C, 80 (2017) 135.
38. Y. Li, X. Liu, X. Liu, N. Mai, Y. Li, W. Wei, Q. Cai, *Colloids. Surf*. B, 88 (2011) 402.
39. X. Li, W. Hou, Y. Song, T. Zhan, X. Wang, *Sens. Actuators* B, 228 (2016) 101.
40. J. Liu, W. Weng, H. Xie, G. Luo, G. Li, W. Sun, C. Ruan, X. Wang, *ACS Omega*, 4 (2019) 15653.
41. N. Lu, N. Y. Gao, X. Huang, *J. Hunan University*, 36 (2009) 64